Rapid Irreversible G Protein Alpha Subunit Misfolding Due to Intramolecular Kinetic Bottleneck that Precedes Mg^{2+} "Lock" after GTP/GDP Exchange†

Bogumil Zelent, Yuri Veklich,‡ John Murray,‡ John H. Parkes, Scott Gibson, and Paul A. Liebman*

Departments of Biochemistry and Biophysics and of Cell and Developmental Biology, University of Pennsylvania Medical Center, Philadelphia, Pennsylvania 19104-6059

Received February 7, 2001; Revised Manuscript Received May 10, 2001

ABSTRACT: Stoichiometric exchange of GTP for GDP on heterotrimeric G protein α (G_α) subunits is essential to most hormone and neurotransmitter initiated signal transduction. G_αs are stably activated in a Mg^{2+} complex with GTPγS, a nonhydrolyzable GTP analogue that is reported to bind G_α with very high affinity. Yet, it is common to find that substantial amounts (30−90%) of purified G proteins cannot be activated. Inactivatable G protein has heretofore been thought to have become "denatured" during formation of the obligatory nucleotide-free or empty (MT) G_α-state that is intermediary to GDP/GTP exchange at a single binding site. We find G_α native secondary and tertiary structure to persist during formation of the irreversibly inactivatable state of transducin. MT G_α is therefore irreversibly misfolded rather than denatured. Inactivation by misfolding is found to compete kinetically with protective but weak preequilibrium nucleotide binding at micromolar ambient GTPγS concentrations. Because of the weak preequilibrium, quantitative protection against G_α aggregation is only achieved at free nucleotide concentrations 10−100 times higher than those commonly employed in G protein radio-nucleotide binding studies. Initial GTP protection is also poor because of the extreme slowness of an intramolecular G_α refolding step (isomerization) necessary for GTP sequestration after its weak preequilibrium binding. Of the two slowly interconverting G_α·GTP isomers described here, only the second can bind Mg^{2+}, "locking" GTP in place with a large net rise in GTP binding affinity. A companion G_α·GDP isomerization reaction is identified as the cause of the very slow spontaneous GDP dissociation that characterizes G protein nucleotide exchange and low spontaneous background activity in the absence of GPCR activation. G_α·GDP and G_α·GTP isomerization reactions are proposed as the dual target for GPCR catalysis of nucleotide exchange.

G protein coupled receptor signal transduction begins when an activated receptor catalyzes amplified exchange of GTP for GDP on G_α[1] subunits of previously quiescent G proteins (*1*−*4*). G proteins are also activated spontaneously by GTP or one of its nonhydrolyzable analogues. Mechanistic study including determination of stoichiometry, binding affinity and kinetics of nucleotide interaction with G_α has traditionally utilized incubation of purified subunits with radioactive nucleotide followed by filtration and counting of labeled protein on nitrocellulose filters (*5*). Low ($\sim 10^{-6}$ M) nucleotide concentration is commonly used in such studies. High reported nucleotide binding affinity (10^8−10^{11} M^{-1}) for the protein (*6*, *7*) is assumed to make larger amounts unnecessary. High background noise due to nonspecific binding of excess free radioactive nucleotide to the filters normally interdicts the use of higher experimental nucleotide concentrations.

Reported activity recovery upon purification differs with type of G protein, but GTP binding may account for as little as 10% of total protein determined by Bradford or UV absorbance assay (*8*, *9*). Such deficiencies have been intuitively attributed to protein denaturation (*8*, *10*) associated with the nucleotide-free (MT) state of G_α that must transiently exist between release of old and binding of new nucleotide at a single nucleotide binding site. Study of the origin and control of the irreversibility of this MT state has previously received little formal attention. Nevertheless, most previous work has used the filter binding method (*6*−*8*, *11*−*14*) to determine G_α-nucleotide equilibrium binding constants as ratios of forward to back rate constants and for other studies. Though G_α activity loss has often been referred to, corrections to kinetic determinations have rarely been made. Instead, incomplete recovery of G protein activity has generally been accepted as irreducible damage control (*8*, *9*).

Crystal structures of a number of G proteins show substantial relocation of a structurally central tryptophan residue (Trp207 in transducin) that accompanies G_α activation (*15*−*18*). The structure change is accompanied by a remarkably large increase in tryptophan fluorescence emission intensity. Increased intrinsic tryptophan fluorescence accompanying G_α activation provides an alternative method for study of nucleotide exchange, GTP′ase activity, and Mg^{2+}

† P.A.L. is supported by NIH Grants EY00012 and EY01583, and Y.V. and J.M. are supported by Fogarty grant FO6TWO2191 and HL30954.

* To whom correspondence should be addressed. Phone: (215) 898-6917. Fax: (215) 573-8093. E-mail: liebmanp@mail.med.upenn.edu.

‡ Cell and Developmental Biology.

[1] Abbreviations: *, **, kinetically distinguishable conformers of G_α·GTPγS; G_α, heterotrimeric G protein α subunit; $G_{t\alpha}$, transducin; MT G_α, nucleotide free G_α; G_α^0, irreversibly misfolded MT G_α; G_α·GDP, G_α with noncovalently bound GDP; GPCR, G protein coupled receptor; GTPγS, guanosine 5′-*O*-(3-thiotriphosphate); ANS, anilino-naphthalene-sulfonate; EDTA, ethylenedinitrilo-tetraacetic acid; DTT, dithiothreitol; R*, activated rhodopsin.

10.1021/bi010272u CCC: $20.00
Published on Web 07/17/2001

dependence of these important signaling proteins (*6*, *11*, *19*−*22*). Increases and decreases in fluorescence intensity correlate quantitatively with radioactive GTP binding and hydrolysis (*20*). However, previous studies have not exploited the additional power of intrinsic tryptophan fluorescence (*23*) to probe intramolecular reaction mechanism of G_α nucleotide exchange and activation (*20*).

It is universally assumed that G_α activation occurs through binding of GTPγS/Mg^{2+} as a complex following GDP dissociation. While this mode of nucleotide binding is known for some ATP binding reactions, it has not heretofore been specifically investigated for heterotrimeric GTP binding proteins. Separate actions of Mg^{2+} and GTPγS on G_α tryptophan fluorescence were noted in earlier work (*21*) but intramolecular intermediates during nucleotide binding were not specifically suggested. A role for intermediates in understanding G protein activation mechanism or activity decay could not therefore be previously appreciated. Consequently, the puzzling discrepancy between reputedly strong GDP and GTPγS/Mg^{2+} binding stability of G_α and activity loss during preparation, storage, and GDP/GTP exchange experiments could not heretofore be rationalized. Neither has it been easy to obtain good estimates of binding constants using either equilibrium or kinetic ratio methods (*24*) without simultaneously making corrections for activity loss in view of the kinetic difficulties described below. Even the powerful ligand binding attributed to GTPγS/Mg^{2+} is incapable of reversing inactivation of "dead" protein. It is therefore not surprising that inactivatable G protein has been regarded as "denatured".

The ability to investigate local structure changes during activation via reaction progress recording in real time using intrinsic tryptophan fluorescence makes possible examination of G protein activation kinetics and magnitude during spontaneous nucleotide exchange with a level of detail inaccessible to other methods. Higashijima et al. (*21*, *22*) used this approach to record G_α nucleotide binding and GTP′ase rates. We have further sharpened the approach by using 295 nm excitation instead of the shorter wavelengths in order to reduce background emission and to emphasize events that may be associated with structural intermediates. We thus obtain larger dynamic changes that are more selective, e.g., for events near tryptophan 207 in transducin. Improvement in quantitative interpretation was also made possible through use of G_α shown to be initially 100% active by another functional method (*25*). This allowed us to calibrate and track molar amounts of G_α activation and deterioration events at different GTPγS and Mg^{2+} ligand concentrations.

In this report, we use real time kinetic analysis of tryptophan fluorescence changes to probe the mechanisms of activation, activity preservation, and inactivation of transducin from bovine retinal rods. We find quantitative G_α preservation to require the presence of free GTP concentration close to a million times higher (~50 μM) than that required (50 pM) for receptor-catalyzed thermodynamic equilibrium (*7*). At lower nucleotide concentrations, kinetic competition for the fate of MT G_α by an irreversible polymerization pathway permanently prevents further nucleotide binding and is responsible for rapid activity loss. Kinetic separation of the roles of GTPγS from Mg^{2+} in the present work suggests a mechanism of ordered sequential binding of GTP before Mg^{2+}. A priori arguments that binding in vivo might nonetheless use the more available GTP/Mg^{2+} complex are not strong since Mg^{2+} has only modest (10^4 M^{-1}) affinity for ATP or GTP. This means that about 0.5 mM of both Mg^{2+} and GTP remain free at 3 mM total intracellular concentration of each.

EXPERIMENTAL PROCEDURES

Transducin ($G_{t\alpha}$) was isolated from rod outer segments of fresh bovine retinas collected from a local slaughterhouse. G_α·GDP and $G_{\beta\gamma}$ were separated using Blue Sepharose chromatography (*26*). Slight modifications of this method also yielded pure G_α·GTPγS·Mg^{2+} (*27*). Purified G protein was concentrated to about 100 μM for storage in pH 7, 10 mM potassium phosphate buffer. The latter assured maximum transparency for quantitative UV spectrophotometric determination of protein concentration and for UV circular dichroism studies. Stored proteins were neither augmented with nucleotide nor with Mg^{2+} after purification and final concentration steps. Proteins were stored in 100 μL or smaller volumes that were flash frozen and kept in liquid nitrogen.

Guanine nucleotides, obtained from Boehringer Mannheim, were purity checked by C18 reversed-phase ion pairing HPLC. Concentration was determined by UV spectroscopy using $\epsilon_{253} = 13\,700$ M^{-1} cm^{-1}. G_α·GDP concentration was assayed using $\epsilon_{276} = 36\,700$ M^{-1} cm^{-1} and was determined to be 100 ± 5% active by quantitative analysis of metarhodopsin II enhancement (*25*) upon reconstitution of G_α plus pure $G_{\beta\gamma}$ with dark, hypotonically stripped, rod outer segment disk membranes. The molar tryptophan fluorescence amplitude of G_α·GDP and of G_α·GTPγS·Mg^{2+} determined in companion experiments was also found to be a good secondary measure of protein stoichiometric functional integrity. MAXC (C. Patton, Hopkins Marine Station) was used to calculate free Mg^{2+} in the presence of EDTA while taking into account the effects of temperature, pH, PO_4 binding and ionic strength.

Fluorescence kinetic measurements were made using 295 ± 0.5 nm excitation and 350 ± 10 nm emission light to exclude spectroscopic changes other than those directly due to tryptophan. GDP dissociation was initiated by dilution of 100 μM stock G_α·GDP to its final 0.5 μM concentration in assay medium consisting of pH 7, 10 mM potassium phosphate, 10 mM DTT, 100 mM KCl, 0.1 mM EDTA, and 2 mM $MgCl_2$ (Mg^{2+}-containing medium), or pH 7, 10 mM potassium phosphate with 10 mM DTT and 7 mM EDTA to reduce the free Mg^{2+} concentration to below 10^{-9} M (Mg^{2+}-free medium). All experiments were conducted at 35 °C, except where noted. Media were carefully particle filtered and bubbled with argon before use. Stoppered, nonfluorescent, quartz (Ultrasil) cuvettes were used throughout. Kinetic constants from experiments yielding simple exponential data were determined using Origin software (OriginLab Corporation, Northampton, MA). Kinetic data in Figure 1 were fit to a double exponential, and the maximum amplitudes that would have been obtained had there been no decay were plotted against GTPγS concentration. These points were then fit to a hyperbolic saturation function, which determined K_D. Though the mathematical function fits to the data are superimposed as continuous curves on all of the figures, they fit the data so accurately as to be nearly invisible under the individual data plots without display in color.

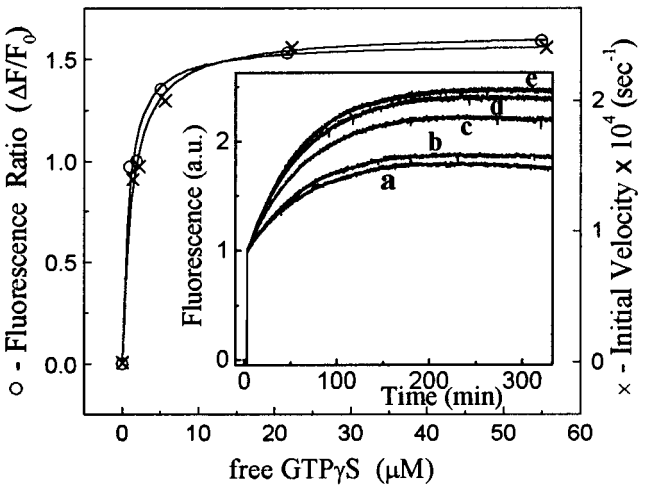

FIGURE 1: (Insert) G_α·GDP diluted to 0.5 μM in preequilibrated 35 °C Mg^{2+}-containing medium with, respectively, (a) 1.2 μM, (b) 2 μM, (c) 5 μM, (d) 20 μM, or (e) 50 μM GTPγS. Initial jump is G_α·GDP fluorescence at time zero. All curves fitted to $y = y_0 + A(e^{-\alpha t} - e^{-\beta t})$ gave a constant value of β (rise time) while α fell (indicating increased stability) with increasing free GTPγS. (Main figure, left axis.) Maximal fluorescence increase (right axis). Initial rate of fluorescence increase. $K_d = 0.8-1.2$ μM for each measure. Curves are hyperbolic saturation fits to the data points. Bound GTPγS was subtracted from total to obtain free GTPγS plotted in the figure.

RESULTS

Full G_α Activation Requires High GTPγS Concentration. G_α·GDP was diluted directly from concentrated stocks into media containing GTPγS in order to avoid deterioration that begins immediately with preincubation in the absence of nucleotide. An initial G_α·GDP fluorescence pedestal was followed by kinetic curves of increasing tryptophan fluorescence intensity whose amplitudes and initial velocities saturated hyperbolically with free GTPγS concentration (K_d of 0.8−1.2 μM GTPγS; 20−50 μM "saturating", see Figure 1). Fluorescence intensity decreased slightly after reaching maximum, particularly at the lowest GTPγS concentrations. This systematic behavior was well fitted at any GTPγS concentration by the equation, $y = y_0 + A(e^{-\alpha t} - e^{-\beta t})$. Fits gave a constant rise time, β^{-1}, for all GTPγS concentrations while α^{-1}, the time constant for the falling phase, became more negligible with increasing GTPγS concentration. The tendency to reach maximum fluorescence at slightly earlier times at lower GTPγS concentrations was entirely explained by the effect on the overall temporal envelope of the decay constant, α, which increases with decreasing GTPγS. The rate of fluorescence increase at early times matched our previous measurements of the time course of GTPγ^{35}S binding at several temperatures from 20 to 40 °C (radiolabel data not shown here but see results of Figure 5B, below). Similar methodological validation of the tryptophan fluorescence method has been reported at single temperatures for $G_{i\alpha}$ and $G_{o\alpha}$ (*21*). Nucleotide exchange rate constants for our fluorescence data agreed closely with those of other studies on $G_{t\alpha}$ at common temperatures (*28*, *29*).

In experiments initiated near 1 μM GTPγS, where fluorescence maxima of lower intensity were attained, subsequent addition of 50 μM GTPγS caused no further fluorescence increase (data not shown but see Figure 2). This implies that at low GTPγS concentration, those G protein molecules that fail to contribute to the higher fluorescence found, e.g., with 50 μM GTPγS present at time zero, had already irreversibly lost their ability to react.

The kinetics of GTPγS-induced fluorescence increase is consistent with previous studies (*8*) that showed GDP dissociation to be rate limiting for GTPγS binding. However, the 2-fold smaller fluorescence transient seen at the lowest GTPγS concentration without a comparable change in rise time (Figure 1, curve a), suggests the presence of a rapid competing reaction pathway that irreversibly removes MT G_α when GDP dissociates from G_α·GDP and before GTPγS binding can preserve it (see Scheme 1). High GTPγS appears to provide mass action and kinetic speed that permits G_α·GTPγS formation to compete effectively with the parallel G_α inactivation path. The two competing reactions are equally effective at about 1μM GTPγS where half-maximal fluorescence activation occurs.

A Single Rate-Limiting Process Controls Speed of GDP Dissociation, GTPγS Binding, and Irreversible G_α Decay. We determined the rate of loss of $G_{t\alpha}$'s ability to be activated by GTPγS more precisely by adding 50 μM GTPγS pulses at various times after GDP dissociation was initiated by G_α·GDP dilution (Figure 2, insert.). As incubation time (GDP dissociation) increased before GTPγS addition, the amplitude and initial velocity of the remaining GTPγS-inducible fluorescence diminished exponentially with 1/*e* time of ca. 90 min. at 35 °C (Figure 2, left axis). This is identical to the time course seen in Figure 1 (rise time, β^{-1}). Thus, G_α's ability to be activated by GTPγS decayed with the same rate constant as that of the fluorescence increase due to binding of GTPγS/Mg^{2+}. This suggests that the same kinetic step (GDP release) rate limits both the rise of fluorescence (activation) in the presence of GTPγS/Mg^{2+} and the loss of ability to rise (inactivatability) in its absence. This is expected if G_α is inactivated quickly upon GDP dissociation with only the remaining G_α·GDP able to be subsequently activated by added GTPγS as its GDP dissociates. Thus, MT-state G_α must rapidly lose its ability to ever again bind GTPγS.

To identify the rate-limiting role of GDP loss kinetics more directly, we determined the amount of G_α·GDP remaining during GDP dissociation in Mg^{2+}-containing medium by adding AlF_4 (30 μM $AlCl_3$ + 10 mM NaF) at various times after G_α·GDP dilution (*30*). AlF_4/Mg^{2+} binds quickly and mimics a third phosphate on any remaining G_α·GDP to form G_α·GDP·AlF_4·Mg^{2+}, a highly fluorescent G_α·GTPγS·Mg^{2+}-like product (*20*, *31*, *32*). We found a 90 min 1/*e* time for loss of G_α·GDP in this experiment (Figure 2, right axis). This matches the kinetics of irreversibility found above.

If any significant amount of MT G_α were to transiently retain GDP binding reversibility, it should be possible to reform some G_α·GDP by adding a pulse of high GDP concentration at any point during the time course of G_α·GDP dissociation. The G_α·GDP found at each time assayed by AlF_4/Mg^{2+} should then be increased compared to that assayed without this extra GDP addition. The results of such an experiment, where 5 min incubation was allowed after injection of an extra 50 μM GDP pulse at various time points before testing with AlF_4/Mg^{2+}, revealed no detectable transient MT G_α that was able to rebind GDP during a dissociation cycle (data not shown). This confirms that MT G_α is rapidly and irreversibly rendered inactive in the absence of a continuously high concentration of GDP (or GTPγS) during G_α·GDP dissociation.

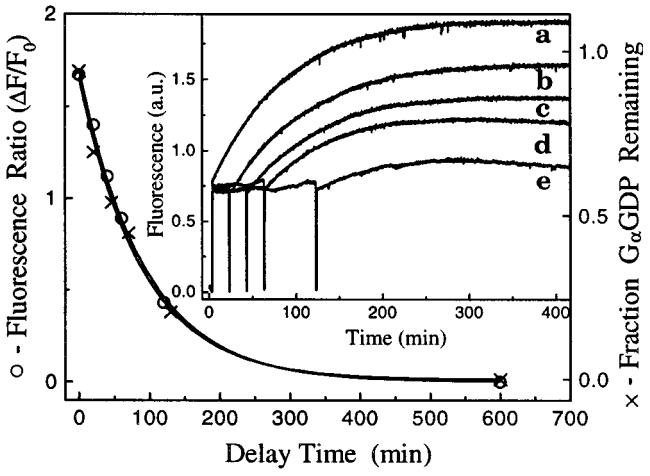

FIGURE 2: (Insert) Fluorescence progress curves show G_α activity diminishes in Mg^{2+}-containing medium as 50 μM GTPγS injection is delayed from (a) 0 min, to (b) 20 min, (c) 40 min, (d) 60 min, or (e) 120 min after G_α·GDP dilution. (Main figure, left axis) Loss of amplitude or initial velocity as function of time delay before GTPγS addition; data taken from insert. (Right axis) AlF_4/Mg^{2+} activatability of G_α·GDP remaining. Both GTPγS activatability and G_α·GDP remaining decreased as a first-order process with 1/*e* time of 90 ± 2 min. In the absence of Mg^{2+}, the results were the same, but with faster 1/*e* time of about 60 min.

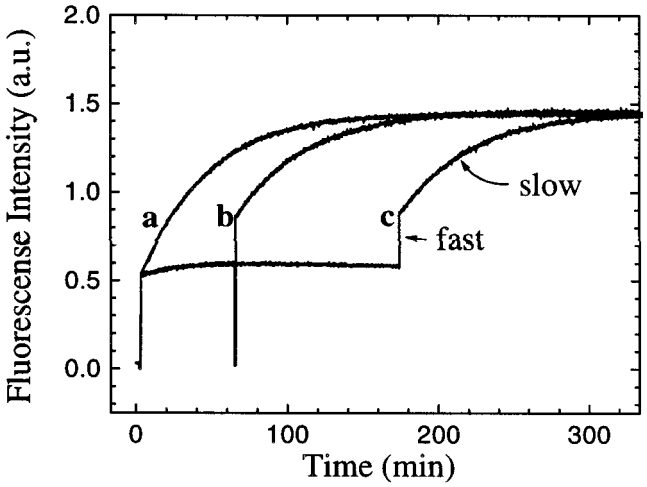

FIGURE 3: G_α·GDP was injected into 50 μM GTPγS-containing Mg^{2+}-free medium. 3.16 mM Mg^{2+} was then injected to give a free [Mg^{2+}] of 0.5 μM; at (a) time zero, (b) 1 h, or (c) 3 h incubation. Note that the fast phase is still increasing slightly from 1 to 3 h.

GTPγS Stabilizes G_α Against Activity Loss in the Absence of Mg^{2+}. We sought to determine whether GTPγS and Mg^{2+} played separate roles in prevention of G_α activity loss. G_α·GTPγS was formed quantitatively from G_α·GDP by incubation with 50 μM GTPγS in the absence of Mg^{2+} ($<10^{-9}$ M) (Figure 3). This caused almost no change in G_α tryptophan fluorescence intensity. Subsequent addition of Mg^{2+}, even after 20 h of GTPγS incubation at 35 °C, could still evoke 88% of the maximum fluorescence seen upon immediate addition of GTPγS/Mg^{2+} to G_α·GDP without preincubation. GDP (50 μM) was also an effective short-term preservative. This shows that occupation of the nucleotide-binding site by either GDP or GTPγS is the critical element in stabilization, requiring no Mg^{2+} per se. Nucleotide concentration must simply be high enough to prevent net loss of G_α into the irreversible kinetic pathway through reversal of weak G_α·GTPγS or G_α·GDP binding, as shown in Figures 1 and 2 (see also Scheme 1).

Multiple G_α·GTPγS States. Addition of Mg^{2+} at various times after initiation of G_α·GTPγS formation from G_α·GDP caused a biphasic fast/slow increase in fluorescence (Figure 3). The fast/slow ratio increased from zero at time zero up to a maximum of about 0.4 as GTPγS incubation time increased before Mg^{2+} addition. This ratio could not be further increased by very long GTPγS incubation time or by higher concentration of GTPγS used in the incubation or higher concentration of Mg^{2+} in the pulsed addition. This suggested that the fast and slow components might represent interconversion between two intramolecular equilibrium forms of G_α·GTPγS, the fast, Mg^{2+}-responding component arising slowly from an antecedent Mg^{2+}-insensitive isomer. The fast fluorescence increase would be due to rapid binding of Mg^{2+} to the penultimate isomer G_α·GTPγS* (see Scheme 1). The slow phase would be due to intramolecular relaxation (isomerization) from G_α·GTPγS that cannot bind Mg^{2+}, to G_α·GTPγS* that can rapidly bind Mg^{2+} (see Scheme 1). The latter yields the high affinity, high fluorescence G_α·GTPγS**·Mg^{2+} complex. Early during incubation, the fast phase is not seen at all since G_α·GTPγS* has not yet formed from G_α·GTPγS. G_α·GTPγS is the product of the initial GTPγS preequilibrium binding reaction.

Figure 4A shows corroborative experimental evidence for intramolecular G_α·GTPγS activation intermediates without the possibly complicating persistence of the GDP released during G_α·GDP dissociation. Here, we initiated the reaction sequence with pure G_α·GTPγS**·Mg^{2+}. This species initially gives the same high fluorescence amplitude per mole of protein as that achieved by conversion of G_α·GDP to G_α·GTPγS**·Mg^{2+} under conditions of high GTPγS with Mg^{2+} shown in Figures 1 and 3. When injected into medium containing 7mM EDTA, G_α·GTPγS**·Mg^{2+}'s high initial fluorescence slowly declines, as Mg^{2+} is released and is

Scheme 1: Model Showing Hypothesized Steps in Interaction of G_α with GDP, GTPγS, and Mg^{2+} [a]

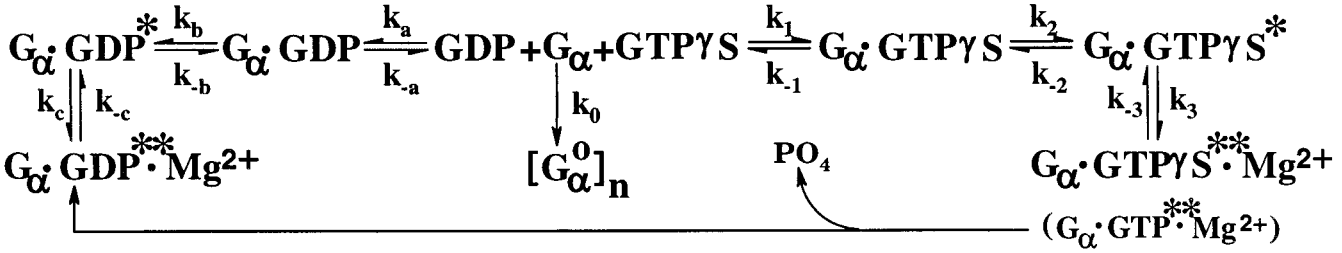

[a] Evidence for reactions proceeding to the right of G_α·GDP are given in the text. Justifications for reactions shown to the left are explained in the Discussion.

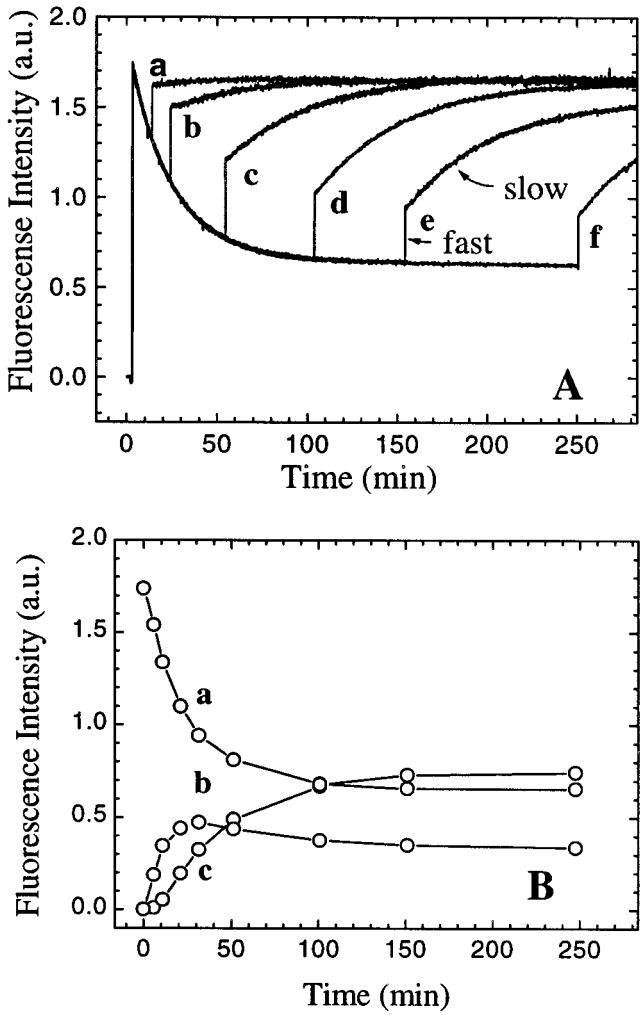

FIGURE 4: (A) Recovery after exponential loss of G_α·GTPγS**·Mg^{2+} fluorescence upon injection into Mg^{2+}-free medium containing 50 μM GTPγS to prevent net G_α·GTPγS dissociation. 3.16 mM Mg^{2+} was subsequently injected to give 0.5 μM free Mg^{2+} at (a) 10 min, (b) 20 min, (c) 50 min, (d) 100 min, (e) 150 min, and (f) 250 min. Note changing ratio of fast to slow recovery phases. (B) Individual component amplitudes taken from panel A at times a−f. (a) Exponential loss of G_α·GTPγS**·Mg^{2+} fluorescence as EDTA removes Mg^{2+}, as shown in panel A; (b) fast phase (G_α·GTPγS*) amplitudes; and (c) Slow phase (G_α·GTPγS $\rightleftharpoons$ G_α·GTPγS*) amplitudes resulting from reintroduction of Mg^{2+}. Note delayed formation of slow phase due to slow G_α·GTPγS* $\rightleftharpoons$ G_α·GTPγS formation before Mg^{2+} induced reversal.

complexed by EDTA, finally reaching the Mg^{2+}-free (10^{-9} M Mg^{2+}) low fluorescence level seen in Figure 3 where G_α·GDP and GTPγS were mixed in the absence of Mg^{2+}.

Reinsertion of Mg^{2+} at various times during the EDTA-induced exponential fluorescence decline causes fluorescence recovery, again with a two phase, fast/slow time course. Starting at early times before full Mg^{2+} loss from G_α·GTPγS**·Mg^{2+}, however, the fluorescence increase induced by pulsed reintroduction of Mg^{2+} (Figure 4A) consists almost entirely of fast with little slow phase. This is consistent with the conclusions of Figure 3 (see also Scheme 1), where the G_α·GTPγS* formed slowly from antecedent G_α·GTPγS. In Figure 4A, G_α·GTPγS* is now the initial intermediate formed upon loss of its Mg^{2+} to the EDTA. This isomer is able to immediately rebind Mg^{2+}. This corroborates the view of Figure 3 that such an intermediate will account for the rapid phase of fluorescence increase only after G_α·GTPγS has enough time to slowly form G_α·GTPγS*. Figure 4A shows that the Mg^{2+}-unreactive species, G_α·GTPγS, also forms slowly from G_α·GTPγS*. This is shown by the fact that the initially large fast/slow ratio diminishes slowly as this G_α·GTPγS forms conjointly with the gradual Mg^{2+} loss (seen as decrease of original fluorescence with time in EDTA). Thus, both formation of G_α·GTPγS* from G_α·GTPγS (Figure 3) and the reverse formation of G_α·GTPγS from G_α·GTPγS* (Figure 4) are slow.

To better show the time-dependent relationship between reaction components seen in Figure 4A, the exponential loss of fluorescence in Figure 4A, and the amplitude of the fast and slow components for each Mg^{2+} injection are replotted in Figure 4B. A clear time delay is seen before development of the slow phase (curve c) while the fast phase (curve b) first increases, then diminishes correspondingly from its peak (G_α·GTPγS* is formed from G_α·GTPγS**·Mg^{2+} but not yet lost to G_α·GTPγS) and the steady state is approached (see Scheme 1). Together the two Mg^{2+} response phases, fast and slow (plus the remaining undissociated G_α·GTPγS**·Mg^{2+} of curve a), sum to the total fluorescence of the G_α·GTPγS**·Mg^{2+} state originally present. Since no GDP that might account for part of the kinetics was introduced at any time in this experiment and since we had already shown that very little G_α escapes into the inactivation pathway in the presence of 50 μM GTPγS, evidence again suggests the presence of at least two G_α·GTPγS isomeric states (see Scheme 1).

The experimental results of Figures 3 and 4 thus provide evidence from both ends of the reaction sequence that at least two intermediates exist on the path of GTPγS binding to G_α after GDP release, culminating in the acquisition of Mg^{2+} by the final intermediate. Our Scheme 1 further illustrates how it is possible for G_α to leak away from this reaction path through formation of the irreversible end state, G_α^0, when the concentration of GTPγS is too low to fully populate the first G_α·GTPγS state that has such weak GTPγS binding affinity. G_α^0 is incapable of rebinding either GDP or GTPγS (Figures 1 and 2). The weakly bound G_α·GTPγS complex can readily dissociate to reform the G_α required for the irreversible step when nucleotide concentration is too low to keep this weak G_α·GTPγS preequilibrium binding saturated. *Irreversible G_α deterioration at low nucleotide concentration makes it impossible to titrate a nucleotide binding equilibrium using classic methods such as equilibrium dialysis or nitrocellulose filter binding without concurrent loss of protein activity due to the slow kinetics of refolding of intermediates.* Reversibility of all the ligand binding reactions (those to the right in the Scheme 1) coupled with the irreversibility of MT G_α aggregation, can allow even G_α·GTPγS**·Mg^{2+} to be slowly lost in the presence of low ambient GTPγS concentrations as seen at later times in Figure 1.

State and Fate of MT G_α. In experiments with low GTPγS concentrations where G_α activity loss was not completely protected by nucleotide, we noticed that cuvette contents became increasingly cloudy over time, suggesting that G_α aggregation might be occurring. By contrast, at 50 μM GTPγS, cuvette contents were always clear. Aggregation progress could be seen by recording 90° static light scattering in our fluorometer during GDP dissociation. In a previous study, we determined the increase in GDP dissociation rate

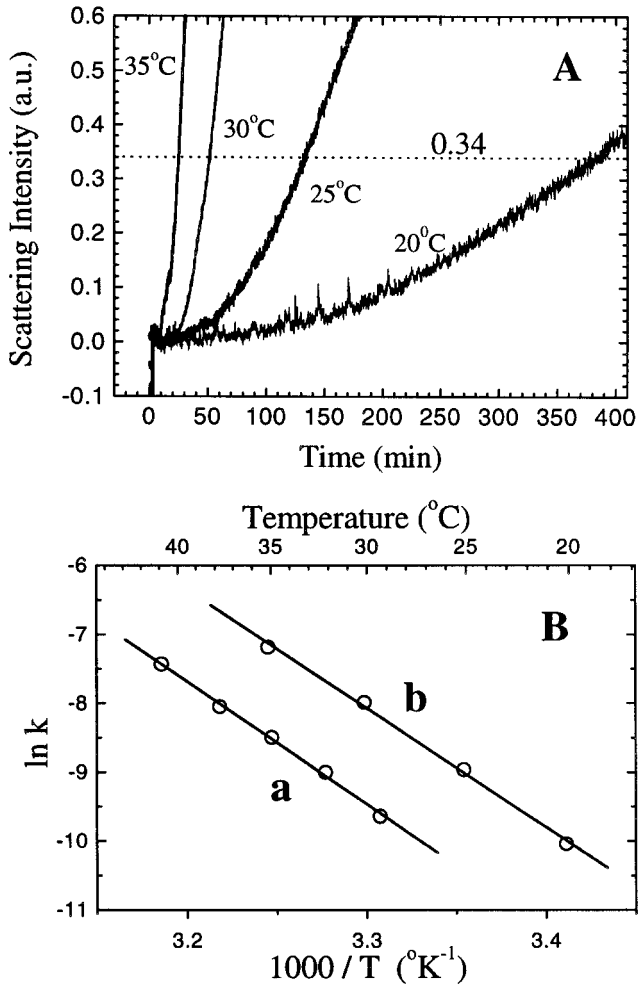

FIGURE 5: (A) 295 nm 90° light scattering increase upon 0.5 μM G_α·GDP dissociation at various temperatures with no GTPγS or GDP added. (B, a) Temperature dependence of reciprocal of time to reach 0.34 scattering intensity increase. (b) Temperature dependence of GDP release rate constant determined as in Figures 1 and 2 or by α^{32}P or γ^{35}S labeled nucleotide exchange. Equal slopes indicate that activation energies are the same for the two processes.

with increasing temperature. We found the thermal dependence of the rate of increase of 90° light scattering (Figure 5A) to have the same Arrhenius slope as that of GDP loss (Figure 5B). Thus, light scattering intensity (aggregation) is intimately coupled to conditions that accelerate GDP loss.

Quantitative quasi-elastic, multiangle, laser light scattering measurements showed that the increasing cloudiness during GDP dissociation was associated with formation in 1 h of a product having a mean molecular weight of about 2.5 MDa, roughly 60 times greater than the monomer mass of G_α. Tungsten shadowing and cryoelectron microscopy of this product showed long monomolecular filaments or irregular, globular particles about 16 nm in diameter, depending on salt conditions. These correspond to about 60 molecules of a protein of 40 kDa mass whose total mass would be about 2.4 MDa. Such particles were absent from controls containing high GTPγS and Mg^{2+}.

MT G_α Is Not Denatured. We further investigated the nature of the irreversibly inactivated state of G_α using circular dichroism, tryptophan emission spectral position (Figure 6), tyrosine-tryptophan resonance energy transfer, scanning calorimetry and ANS binding. In each case, though small

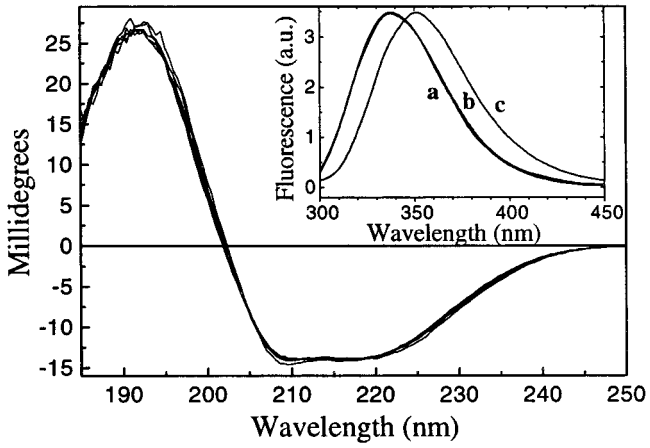

FIGURE 6: Circular dichroism spectra recorded at 10 min intervals over 3 h and averaged in groups to show 30 min intervals (no GDP added, 35 °C). (Insert) Tryptophan fluorescence of G_α·GDP (a) before, (b) after MT G_α formed, and (c) G_α denatured in 6 M guanidine HCl.

systematic changes paralleled the GDP dissociation kinetics, none showed signs of tertiary or secondary structural changes that might be identified as a "denatured" or unfolded state. Instead, small changes more typical of ligand loss and/or protein−protein association were seen. Thus, MT G_α appears similarly to be misfolded rather than denatured.

DISCUSSION

G_α Activity Loss Is Due to Weak Preequilibrium Nucleotide Binding Followed by a Kinetic "Bottleneck" among Ligand-Binding Intermediates. The one micromolar GTPγS K_d found here for activation or "protection" of G_α from irreversible loss of activatability during spontaneous nucleotide exchange, implies that G_α aggregation and GTPγS binding pathways compete at about the same rate for the fate of MT G_α when GTPγS concentration is near one micromolar. Yet, a previously estimated 50 pM GTPγS/Mg^{2+} K_d (*7*) would predict that much lower, near stoichiometric, amounts of nucleotide should have been able to fully complex G_α. What accounts for this discrepancy in apparent nucleotide binding affinities? The first part of the answer appears to be that Mg^{2+}, though essential to the final high affinity of GTPγS binding previously observed, is not involved in the immediate protection of G_α required upon GDP dissociation. Despite the much higher affinity expected of GTPγS/Mg^{2+}, GTPγS alone (Figure 3) protects about as well as GTPγS/Mg^{2+} (Figure 1). This can only be the case if Mg^{2+} fails to accompany GTPγS into the initial G_α·GTPγS preequilibrium binding pocket but rather binds later, after this complex is isomerized (Figure 3). Thus, initial GTPγS binding appears to be Mg^{2+}-insensitive, weak, and readily reversible.

Subsequent isomerization of G_α·GTPγS to G_α·GTPγS* allows Mg^{2+} to bind for the first time. This feature suggests that the Mg^{2+} binding configuration of the protein might even be induced by GTPγS binding as the protein conformation changes to the G_α·GTPγS* form. G_α·GTPγS* formation also effectively removes a fraction of G_α·GTPγS from access to GTPγS aqueous dissociation by placing a high kinetic barrier between isomers. But this same kinetic barrier also slows protective G_α·GTPγS* formation from G_α·GTPγS, making it necessary to use very high GTPγS concentrations to

increase the rate of protective rebinding of GTPγS to G_α through k_1 in competition with formation of irreversible G_α through k_0.

Linked Basic Causes. Thus, weak initial protection of G_α by GTPγS is not entirely due to weak preequilibrium binding. The ~3000 s slowness of isomerization simply fails to remove preequilibrium G_α·GTPγS as G_α·GTPγS* (slow phase, Figure 3 and 4A) before GTPγS dissociation returns it to the G_α aggregation pathway. This failure is in turn related to deferral of the high affinity Mg^{2+} binding step until after G_α·GTPγS* is formed. High affinity Mg^{2+} binding to G_α·GTPγS* ultimately serves as a "magnesium lock" on the nucleotide bound state. But it is not possible to close the lock until the hasp is folded over the staple, i.e., until G_α·GTPγS has folded to generate the G_α·GTPγS* that is capable of being locked by Mg^{2+}. The powerful kinetic bottleneck of slow G_α·GTPγS* formation, compared to the speed of nucleotide dissociation from the G_α·GTPγS preequilibrium complex, explains why neither maximal G_α activation nor protection from activity loss could be achieved at the low GTPγS concentrations previously thought to be saturating. Slow intramolecular conversion of G_α·GTPγS into the Mg^{2+}-binding G_α·GTPγS* configuration leaves preequilibrium G_α·GTPγS vulnerable to repeated cycles of GTPγS binding and dissociation (k_{-1} in Scheme 1). Thus, MT G_α forms repeatedly with opportunities for irreversible loss through aggregation (k_0). Only momentary G_α protection can occur at micromolar GTPγS concentrations through rebinding of GTPγS at a speed of k_1 times the GTPγS concentration.

Preequilibrium binding and intramolecular isomerization intermediates in the mechanism described above (see Scheme 1) are formally similar to those previously described for binding of GDP or GTP to EF-Tu (*34*, *35*) to tubulin or to h-ras (*36*) and for ADP or ATP binding to myosin (*37*) or kinesin. In these cases, also, protein isomerization can kinetically isolate the initial preequilibrium nucleotide-binding complex from dissociation. Macroscopic nucleotide binding rate constants (that would include microscopic constants, k_1 and k_2 of our Scheme 1) are around 10^5 M^{-1} s^{-1} (*36*). This is substantially less than the $>10^8$ M^{-1} s^{-1} bimolecular reaction rate limit seen for the fastest known diffusion-limited binding or reaction of a small ligand (*36*, *38*, *39*). Such low apparent bimolecular rate constants generally imply that a weak bimolecular preequilibrium is concatenated with one or more subsequent slow intramolecular isomerizations. Such concatenations apparently reflect the time required for reconfiguration of the protein to accommodate the ligand (induced fit). This reduces the apparent (macroscopic) bimolecular rate constant (*40*).

Lifetime of the Preequilibrium Complex and Aggregation of G_α. G_α appears to be protected from aggregation only when bound to nucleotide. Each G_α, upon GDP dissociation, faces the problem of slow GTPγS protection (Figure 4) that conspires to trap it into the $G_\alpha{}^0$ path. Neither GDP nor GTP can apparently retain G_α in the initial preequilibrium complex for times sufficiently long compared to MT G_α aggregation unless nucleotide concentration is high enough to provide rebinding events more frequently than aggregation events. What is the duration of G_α protection in the G_α·GTPγS preequilibrium complex before GTPγS dissociates and MT G_α becomes trapped by the $G_\alpha{}^0$ path? Though the GTPγS dissociation rate is not readily measured by present experiments, its order of magnitude can be appreciated as follows: Assume our 1 μM K_d for GTPγS activation is a legitimate macroscopic equilibrium constant, K_1. A forward rate constant, k_1, of 10^5 M^{-1} s^{-1} for GTPγS binding (like that for ATP binding of myosin) would imply $k_{-1} = 10^{-1}$ s^{-1} for GTPγS dissociation. That is, nucleotide would be re-released 10 s, on average, after binding. If k_1 were to approach the 10^8 M^{-1} s^{-1} diffusion limit, k_{-1} would be 10^2 s^{-1} giving a GTPγS preequilibrium protection time of only 10 milliseconds before re-dissociation. Since GTPγS binding and G_α aggregation are in direct competition, G_α, once formed, would be irreversibly inactivated on about this time scale. The overwhelming slowness of G_α·GDP*/G_α·GDP or G_α·GTPγS*/G_α·GTPγS isomerization that rate limits nucleotide dissociation, makes it impossible for us to determine on which end of this brief time scale MT G_α inactivation lies without more specialized approaches.

Relevance of G_α·GTPγS Kinetics to Slowness of G_α·GDP Dissociation. GDP dissociation from G_α·GDP is spontaneous but its very slow rate is essential to the assurance of a low background of G protein activation in the absence of specific GPCR stimulation. What is the cause of this very slow dissociation rate? We propose that a G_α·GDP*/G_α·GDP isomerization kinetic barrier like that described for G_α·GTPγS*/G_α·GTPγS above is the origin of this limit. Crystal structures show the same G_α binding site to accommodate either GDP or GTP. It is not therefore unreasonable to expect similar molecular structures for the Mg^{2+}-free nucleotide binding intermediates in each case. Similarity between such reaction intermediates is represented by the symmetric complexes of G_α with GTPγS and GDP shown in our model. Thus, rules that regulate GTPγS binding and release in the absence of Mg^{2+} may tell us what might be expected during GDP binding and release.

The ratio of fast to slow components in response to pulsed Mg^{2+} addition after saturating GTPγS equilibration shown in Figure 3 gives a G_α·GTPγS*/G_α·GTPγS equilibrium constant of 0.4. Since G_α·GTPγS**·Mg^{2+} formation is fast, there is no reverse reaction and the slow phase of Mg^{2+} action is due to k_2 alone. k_2 is determined to be 3.3×10^{-4} s^{-1}, the reciprocal of the slow exponential rise time of 3000 s. k_{-2} can then be calculated as $k_{-2} = k_2/K_2 = 3.3 \times 10^{-4}$ $s^{-1}/0.4 = 8.3 \times 10^{-4}$ s^{-1} (1200 s). Since k_{-1} is fast compared to k_{-2}, 1200 s would be the characteristic time for G_α·GTPγS* conversion to allow G_α·GTPγS dissociation (and decay through the faster k_0) in the absence of Mg^{2+}.

Macroscopic slowness of GDP dissociation from G_α is expected to similarly involve a slow isomeric (k_{-b}) relaxation, G_α·GDP* $\Leftrightarrow$ G_α·GDP, concatenated with a fast GDP binding/release preequilibrium. In this context, Figure 2 gives a macroscopic GDP off rate constant (k_{-a}) of 2×10^{-4} s^{-1} for transducin at 35 °C. Using this value, together with a macroscopic dissociation constant (K_D) of 25 μM (at 25 °C) (*41*, *42*), we calculate an effective forward rate constant $k_a = k_{-a}/K_D = 8$ M^{-1} s^{-1} as the association rate for binding of GDP to G_α. This tiny value for GDP binding to G_α is even smaller than for EF, tubulin, ras, myosin, kinesin, etc., indicating quite hindered nucleotide binding mechanics and implying a slow intramolecular isomerization step. Binding and release of GDP, like that of GTPγS, is clearly and severely hindered by the presence of an intramolecular isomerization reaction. It thus seems likely that the same

rate-limiting intramolecular isomerization following weak preequilibrium nucleotide binding is responsible for instabilities common to both the GDP and GTPγS protection of G_α from formation of the irreversible state. This reaction is also the basis of the very slow rate of GDP dissociation that is so important to transducin's quiescence in the absence of GPCR activation.

It should be noted that during a GTP′ase cycle, G_α·GDP** then G_α·GDP* are the first intermediates to form after loss of PO_4 from G_α·GTP**·Mg^{2+} (see Scheme 1). G_α·GDP**·Mg^{2+} would be expected to rapidly lose its Mg^{2+} as indicated by the known weak Mg^{2+} effect on GDP dissociation (*6*). The G_α·GDP* isomerization kinetic barrier would then prevent equilibrium with the unstable preequilibrium complex, G_α·GDP, from being realized. Though we are not yet certain what the microscopic equilibrium constant is for this isomerization, it is likely in the interest of parsimony to favor G_α·GDP like that of GTPγS binding favors its G_α·GTPγS preequilibrium complex. This would be advantageous for R* catalysis since it allows equilibrium to be realized in the forward direction appropriate to signal transduction. We propose that G_α·GDP* is the intermediate that binds $G_{\beta\gamma}$ upon GTP hydrolysis.

Nucleotide Binding Intermediates and Mechanism of GDP/GTP Exchange Catalysis by GPCRs. Activated rhodopsin accelerates G protein nucleotide exchange from a 2×10^{-4} s^{-1} spontaneous rate to its $1-5 \times 10^3$ s^{-1} catalytic rate (*43*), an acceleration of some 10^7-fold. Lower spontaneous rates at lower temperature can give even higher catalytic ratios near 10^8. Mechanistic reaction steps in nucleotide exchange that would be accelerated by R* have not previously been proposed. What reaction steps in our model are likely to be catalyzed? The model clearly indicates two rate-limiting reaction steps that must be accelerated. These are the slow G_α·GDP* $\leftrightarrow$ G_α·GDP and G_α·GTPγS $\leftrightarrow$ G_α·GTPγS* isomerizations. R* (and GPCRs in general) must act operationally as a dual catalyst that mediates these two (nucleotide exchange) reactions in rapid succession. That is, R* must first catalyze refolding of G_α·GDP*, the isomer from which GDP cannot escape, into G_α·GDP, the preequilibrium complex from which GDP may escape rapidly without needing any help from catalysis. If the G_α·GDP* equilibrium already favors G_α·GDP, catalysis could cause immediate diffusion-limited GDP dissociation. The necessary catalytic speed that would allow diffusion-limited dissociation can be estimated. For instance, with a GDP-dissociation K_a of 10^{-5} M, diffusion-limited GDP binding to form the preequilibrium complex, G_α·GDP, implies a GDP dissociation rate of $k_{-a} = k_a K_a = 10^8$ M^{-1} $s^{-1} \times 10^{-5}$ $M = 10^3$ s^{-1}, a value very near the overall amplification rate observed for R* catalysis of G protein activation in vision (*4*). To achieve this rate requires R* to lower the kinetic activation barrier so that the isomerization reaction is still faster than this aqueous diffusion rate limit during R* action. A faster diffusion-limited rate could be achieved if GDP's K_a were even weaker. Thus, $K_a = 10^{-4}$ M would give $k_{-a} = 10^4$ s^{-1}. That is, R* acts by causing k_{-b} to increase from $\sim 10^{-4}$ s^{-1} to 10^3 s^{-1} to achieve the catalytic rate increase of 10^7-fold.

GTP binding would need to be faster than GDP dissociation to allow the latter to continue to be the single rate-limiting step in amplification. Using the same approach as for GDP above, 10^{-3} M cytoplasmic GTP concentration could yield an aqueous diffusion-limited GTP binding rate near 10^8 M^{-1} $s^{-1} \times 10^{-3}$ $M = 10^5$ s^{-1} or 10 μs per GTP binding event. Mg^{2+} binding would then need to be similarly quick to continue to maintain GDP release as the rate-limiting step. This is clearly possible given a 3 mM free cytoplasmic Mg^{2+} concentration plus electro-diffusional acceleration by the negative membrane potential. An important prediction of these identifications in our reaction model is that R* catalysis of nucleotide exchange will not require Mg^{2+} per se, though release of activated G_α from $G_{\beta\gamma}$ and receptor might. Failure of $G_{\beta\gamma}$ release from G_α with reduced effector activation was associated with primary Mg^{2+} binding deficiency in the G226A $G_{s\alpha}$ mutant (*11*). Accelerated GTPγS dissociation (due to weak Mg^{2+} affinity) but no change in GTPγS binding rate also accompanied this change. These observations are completely consistent with the role of Mg^{2+} illustrated in our model.

A companion argument can be made against estimates of a GDP dissociation constant near 10^{-8} M for transducin (*44*). Thus, $k_{-a} = k_a K_a = 10^8$ M^{-1} $s^{-1} \times 10^{-8}$ $M = 1$ s^{-1} would be the fastest GDP could escape for a K_a of 10^{-8} M. This is clearly an unrealistically low rate of dissociation for vision, a physiologic process that requires near 1000 G protein activation events per receptor per second. On the other hand, it might be perfectly compatible with slower signaling mechanisms that require little amplification.

Cytoplasmic free nucleoside triphosphates are maintained at multi-millimolar concentrations, nearly 100-fold higher than those of the diphosphates (*45*). Thus, GTP binding by G_α is thermodynamically spontaneous. Signal-initiated "switching" would not be possible without sustained quiescence of G_α·GDP until GPCR activation. This quiescence needs to be assured by kinetic stability of G_α·GDP* that prevents easy spontaneous dissociation rather than by sustained thermodynamic ligand saturation of G_α·GDP. The combination of spontaneous GDP dissociation, energetic binding of Mg^{2+}, and GTP and the spontaneous hydrolysis of GTP drives a continuous G_α/nucleotide exchange cycle that can only be controlled by kinetic barriers (see Scheme 1). These barriers are identified here for the first time as protein isomerizations between nucleotide binding intermediates.

What Is the Physical Basis of Aggregation? The G_α molecular surfaces involved in MT state aggregation are not yet mapped. However, recombinant unmyristoylated $G_{i\alpha}$, as well as Lys C proteolyzed $G_{t\alpha}$ that lacks its N-myristoylation with 25 N terminal amino acid residues (*46*), was also found to aggregate upon GDP loss, showing that a lipophilic N terminus is not essential to aggregation. Nucleotide is held between helical and GTP′ase domains of G_α (*15*, *32*). Each domain interface of G_α may have the opportunity to associate with the complimentary surface of another G_α molecule instead of with its own intramolecular companion-domain, initiating chain polymerization in the MT state. We could not block such polymer formation by using excess recombinant $G_{s\alpha}$ (*47*) or $G_{t\alpha}$ helical domains to compete with aggregation. Excess $G_{\beta\gamma}$ reduced the aggregation rate minimally but this may have resulted from its ability to decrease the rate of GDP loss from G_α·GDP (*6*). Aggregation is accelerated by high ionic strength and specifically by Ca^{2+} and Mg^{2+}. Electrostatic neutralization or shielding of surface charges would leave several highly exposed surface hydrophobic patches on G_α vulnerable to interaction with similar

patches on other G_α molecules (*15*, *32*).

Irreversible Misfolding upon Ligand Loss Could be a More General Protein Phenomenon. Evidence for an early G_α·GTPγS binding intermediate with later Mg^{2+} stabilization can perhaps also be found in the prescient work of Higashijima, et al. (*21*), suggesting that the same mechanistic considerations apply to G_i. and G_o. Understanding of the structure of MT G_α will certainly have further implications for what an activated receptor must do to ensure survival of this obligatorily unstable ligand-less intermediate configuration during the nucleotide exchange catalyzed by all G protein coupled receptors.

The mechanisms that we describe may provide further insight into the molecular pathology of diseases such as, e.g., pseudohypoparathyroidism, type Ia (PHP-Ia) where a single somatic mutation accelerates spontaneous G_s·GDP dissociation. This mutation causes endocrine hyperfunction or hypofunction (*48*), depending on temperature-dependent competition between the accelerated G protein activation (GTP binding) that is associated with more frequent GDP dissociation and the "denaturation" which we would here reinterpret as misfolding and aggregation.

Our model also helps explain the destabilization of the G226A $G_{s\alpha}$ mutant that fails to bind Mg^{2+} tightly and at the same time exhibits weak GTPγS affinity (*11*). Each of the above mutants might be seen as variants of the normal reaction sequence of this model with particular intermediate rate or binding constants altered by the mutated structure in a manner that should be measurable through approaches described here and subsequently.

Nucleotide and other small ligand binding proteins such as kinases should depend partly on ligand binding energy for their conformational stability. These may be similarly subject to misfolding during transient ligand cycling on their own particular time scales. In the temporary absence of ligand stabilization, these too may generate misfolded conformations that may aggregate as has already been seen for tubulin (*49*) or actin (*50*).

Misfolding due to loss of ligand from either native or mutant proteins might have broader implications for disease or aging mechanisms associated with formation of misfolded protein aggregates (plaques) like those of, e.g., amyloid, Alzheimer's or prion disease (*33*, *51*). Since the physiologic function of few such proteins is yet known, it is possible that some may be extremely sensitive to the stabilization provided by native ligands.

ACKNOWLEDGMENT

We thank Dr. Mark Lemmon for assistance with multi-angle laser light scattering measurements, Dr. Henry Bourne for gifts of $G_{s\alpha}$ helical and GTP′ase domain expression constructs, Dr. Heidi Hamm for recombinant $G_{i\alpha}$, Drs. William DeGrado, Steven Betz, Joel Schneider, and R. Blake Hill for assistance with circular dichroism studies, Dr. John Weisel for suggesting an EM approach and Dr. James Lear for providing important suggestions that sharpened interpretations of our findings. Nancy Thornton, Bob Sharp, and Christina Reilly provided expert preparative and technical assistance.

REFERENCES

1. Cassel, D., and Selinger, Z. (1978) *Proc. Natl. Acad. Sci. U.S.A. 75*, 4155−4159.
2. Fung, B. K.-K., and Stryer, L. (1980) *Proc. Natl. Acad. Sci. U.S.A. 77*, 2500−2504.
3. Yee, R., and Liebman, P. A. (1978) *J. Biol. Chem. 253*, 8902−8909.
4. Liebman, P. A., and Pugh, E. N., Jr. (1982) *Vis. Res. 22*, 1475−1480.
5. Godchaux, W. III, and Zimmerman, W. F. (1979) *J. Biol. Chem. 254*, 7874−7884.
6. Higashijima, T., Ferguson, K. M., Sternweis, P. C., Smigel, M. D., and Gilman, A. G. (1987) *J. Biol. Chem. 262*, 762−766.
7. Malinski, J. A., Zera, E. M., Angleson, J. K., and Wensel, T. G. (1996) *J. Biol. Chem. 271*, 12919−12924.
8. Ferguson, K. M., Higashijima, T., Smigel, M. D., and Gilman, A. G. (1986) *J. Biol. Chem. 261*, 7393−7399.
9. Hepler, J. R., Kozasa, T., Smrcka, A. V., Simon, M. I., Rhee, S. G., Sternweis, P. C., and Gilman, A. G. (1993) *J. Biol. Chem. 268*, 14367−14375.
10. Faurobert, E., Otto-Bruc, A., Chardin, P., and Chabre, M. (1993) *EMBO J. 12*, 4191−4198.
11. Lee, E., Taussig, R., and Gilman, A. G. (1992) *J. Biol. Chem. 267*, 1212−1218.
12. Yamanaka, G., Eckstein, F., and Stryer, L. (1985) *Biochemistry 24*, 8094−8101.
13. Smigel, M., Katada, T., Northrup, J. K., Bokoch, G. M., Ui, M., and Gilman, A. G. (1984) *Adv. Cycl. Nucleotide Protein Phosphorylation Res. 17*, 1−18.
14. Northup, J. K., Smigel, M. D., and Gilman, A. G. (1982) *J. Biol. Chem. 257*, 11416−11423.
15. Noel, J. P., Hamm, H. E., and Sigler, P. B. (1993) *Nature 366*, 654−663.
16. Lambright, D. G., Noel, J. P., Hamm, H. E., and Sigler, P. B. (1994) *Nature 369*, 621−628.
17. Coleman, D. E., and Sprang, S. R. (1998) *Biochemistry 37*, 14376−14385.
18. Coleman, D. E., Lee, E., Mixon, M. B., Linder, M. E., Berghuis, A. M., Gilman, A. G., and Sprang, S. R. (1994) *J. Mol. Biol. 238*, 630−634.
19. Lan, K. L., Remmers, A. E., and Neubig, R. R. (1998) *Biochemistry 37*, 837−843.
20. Phillips, W. J., and Cerione, R. A. (1988) *J. Biol. Chem. 263*, 15498−15505.
21. Higashijima, T., Ferguson, K. M., Sternweis, P. C., Ross, E. M., Smigel, M. D., and Gilman, A. G. (1987) *J. Biol. Chem. 262*, 752−756.
22. Higashijima, T., Ferguson, K. M., Smigel, M. D., and Gilman, A. G. (1987) *J. Biol. Chem. 262*, 757−761.
23. Lakowicz, J. R. (1999) *Principles of Fluorescence Spectroscopy*, 2nd Ed., Kluwer Academic/Plenum Publishers, New York.
24. Goody, R. S., Frech, M., and Wittinghofer, A. (1991) *Trends Biochem. Sci. 16*, 327−328.
25. Parkes, J. H., Gibson, S. K., and Liebman, P. A. (1999) *Biochemistry 38*, 6862−6878.
26. Pines, M., Gierschik, P., Milligan, G., Klee, W., and Spiegal, A. (1985) *Proc. Natl. Acad. Sci. U.S.A. 82*, 4095−4099.
27. Kroll, S., Phillips, W. J., and Cerione, R. A. (1989) *J. Biol. Chem. 264*, 4490−4497.
28. Fawzi, A. B., and Northup, J. K. (1990) *Biochemistry 29*, 3804−3812.
29. Ramdas, L., Disher, R. M., and Wensel, T. G. (1991) *Biochemistry 30*, 11637−11645.
30. Sternweis, P. C., and Gilman, A. G. (1982) *Proc. Natl. Acad. Sci. U.S.A. 79*, 4888−4891.
31. Bigay, J., Deterre, P., Pfister, C., and Chabre, M. (1985) *FEBS Lett. 191*, 181−185.
32. Coleman, D. E., Berghuis, A. M., Lee, E., Linder, M. E., Gilman, A. G., and Sprang, S. R. (1994) *Science 265*, 1405−1412.

33. Peterson, S. A., Klabunde, T., Lashuel, H. A., Purkey, H., Sacchettini, J. C., and Kelly, J. W. (1998) *Proc. Natl. Acad. Sci. U.S.A. 95*, 12956−12960.
34. Eccleston, J. F. (1984) *J. Biol. Chem. 259*, 12997−13003.
35. Chau, V., Romero, G., and Biltonen, R. L. (1981) *J. Biol. Chem. 256*, 5591−5596.
36. John, J., Sohmen, R., Feuerstein, J., Linke, R., Wittinghofer, A., and Goody, R. S. (1990) *Biochemistry 29*, 6058−6065.
37. Trentham, D. R., Eccleston, J. F., and Bagshaw, C. R. (1976) *Q. Rev. Biophys. 9*, 217−281.
38. Fersht, A. (1999) *Structure and mechanism in protein science: a guide to enzyme catalysis and protein folding*, W. H. Freeman, New York.
39. Eccleston, J., Kanagasabai, T. F., and Geeves, M. A. (1988) *J. Biol. Chem. 263*, 4668−4672.
40. DeLisi, C. (1980) *Q. Rev. Biophys. 13*, 201−230.
41. Panico, J., Parkes, J. H., and Liebman, P. A. (1990) *J. Biol. Chem. 265*, 18922−18927.
42. Kahlert, M., Konig, B., and Hofmann, K. P. (1990) *J. Biol. Chem. 265*, 18928−18932.
43. Liebman, P. A., Parker, K. R., and Dratz, E. A. (1987) *Annu. Rev. Physiol. 49*, 765−791.
44. Zera, E. M., Molloy, D. P., Angleson, J. K., Lamture, J. B., Wensel, T. G., and Malinski, J. A. (1996) *J. Biol. Chem. 271*, 12925−12931.
45. Dawis, S. M., Graeff, R. M., Heyman, R. A., Walseth, T. F., and Goldberg, N. D. (1988) *J. Biol. Chem. 263*, 8771−8785.
46. Mazzoni, M. R., Malinski, J. A., and Hamm, H. E. (1991) *J. Biol. Chem. 266*, 14072−14081.
47. Markby, D. W., Onrust, R., and Bourne, H. R. (1993) *Science 262*, 1895−1901.
48. Iiri, T., Herzmark, P., Nakamoto, J. M., Van Dop, C., and Bourne, H. R. (1994) *Nature 371*, 164−170.
49. Ventilla, M., Canbor, C. R., and Shelanski, M. (1972) *Biochemistry 11*, 1554−1561.
50. De La Cruz, E. M., and Pollard, T. M. (1996) *Biochemistry 35*, 14054−14061.
51. Jarrett, J. T., and Lansbury, P. T., Jr. (1993) *Cell 73*, 1055−1058.

BI010272U